Turkish Journal of Electrical Engineering & Computer Sciences

http://journals.tubitak.gov.tr/elektrik/

Research Article

Turk J Elec Eng & Comp Sci
(2020) 28: 2004 – 2019

doi:10.3906/elk-1909-75

Finite-time dynamic surface approach to nonlinear systems with mismatched uncertainties

Guofa SUN[1], **Yaming XU**[2,*]

[1]School of Information and Control Engineering, Qingdao University of Technology, Qingdao, PR China
[2]School of Astronautics, Harbin Institute of Technology, Harbin, PR China

Received: 13.09.2019 • **Accepted/Published Online:** 09.03.2020 • **Final Version:** 29.07.2020

Abstract: This paper develops a finite-time dynamic surface control (DSC) scheme for nonlinear systems with mismatched uncertainties via a high-order sliding mode(HOSM) observer. By designing a second-order terminal sliding surface based on the estimated signals, an observer-based sliding mode control (SMC) is designed to counteract the mismatched uncertainties in each step of backstepping. The proposed DSC scheme exhibits the following two attractive features. One is the application of HOSM observer to deal with mismatched system uncertainty functions. This is very different from the traditional approximator-based adaptive methods in dealing with high-order uncertain nonlinear systems. The other is the finite-time convergence of the provided algorithm, which guarantees the transient performance of tracking signals. Especially, the finite convergence time is explicitly given in the controller design and stability analysis. Simulation results of numerical example illustrates that the proposed approach shows better control performance than traditional approximators-based adaptive methods.

Key words: High-order siding mode observer, dynamic surface control, extended state observer, finite-time convergence, sliding mode control

1. Introduction

In the past decades, lots of adaptive control schemes have been proposed based on function approximators, such as neural networks (NN) or fuzzy systems (FS), to deal with uncertain nonlinear systems with unknown functions. For instance, Liu et al. [1] developed a NN-based adaptive control strategy of the full state constrained nonlinear systems. Then, Yu et al. [2] extended adaptive neural control to a class of multiple-input multiple-output (MIMO) strict-feedback nonlinear time-delay systems. Alternatively, Qiu et al. [3] considered an adaptive fuzzy control approach for a pure-feedback nonlinear systems with unknown functions and unmeasured states. Similarly, by considering simplified barrier Lyapunov function, Li and Tong [4] addressed the problems of stability and finite-time tracking control for a class of MIMO nonlinear systems with errors constraint and unknown dead zone. The aforementioned results and the references therein solved many nonlinear control problems by employing function approximators to adaptive approximate uncertain system functions. Despite the online estimating of uncertain functions and compensating them, the approximation precision of approximators were not taken into consideration, which definitely affected the closed-loop tracking performance. Fortunately, the reinforcement learning(RL) [5] improved the approximation ability, which resulted in the integral RL from adaptive control in [6]. However, employing the learning ability of approximators to estimate uncertain functions online increased the computation burden and thus the convergence time. In this paper, we will accordingly

*Correspondence: xuyaming2000@163.com

investigate the finite-time observation and finite-time tracking control of nonlinear systems with uncertain nonlinear functions.

Sliding mode control (SMC) was a powerful tool in dealing with uncertain nonlinear systems with matched disturbances. A brief survey on variable structure control systems with sliding modes was presented in [7]. Shi et al. [8] considered the tuning of second-order sliding mode controller with finite-time convergence in single-input-single-output nonlinear systems with uncertainties functions. Alternatively, in [9], a nonlinear sliding surface included initial condition was proposed to alleviate chattering and ensure a smooth control for a rigid spacecraft with external disturbances, where high accuracy and steady state precision was ensured. Furthermore, to improve the control performance, many modified novel SMC has been reported. For instance, in [10], a adaptive SMC scheme with adaptive super twisting algorithm was proposed for robotic manipulators including actuator dynamics. Alternatively, Qiao and Zhang [11] proposed a second-order fast nonsingular terminal sliding mode manifold for dynamic uncertainties and time-varying external disturbances. Furthermore, Feng et al. [12] proposed a integral-type terminal sliding mode observer for estimating the variable of a LI-ion cell, which was used for the real-time estimation on the state-of-charge and state-of-health of lithium-ion (Li-ion) batteries. Then, based on extended state observer (ESO), Wu et al. [13] proposed a nonsingular terminal sliding mode control for a flexible adsorption system by using Lyapunov synthesis. In this paper, we will incorporate second-order terminal SMC into traditional DSC method to develop finite-time control for nonlinear systems with mismatched uncertain functions.

Finite-time control has also been investigated for decades by lots of researchers. For example, in [14], a class of bounded continuous time-invariant finite-time stabilizing feedback laws is given for the double integrator by Bhat and Bernstein. Then, Abooee and Arefi [15] studied the problem of finite-time stabilization for a connected chain of double-integrator systems. Furthermore, Hou et al. [16] developed continuous finite-time control for servo motor systems with terminal sliding mode. Similarly, Yin et al. [17] presented a new fast finite-time integral terminal sliding-mode for force tracking control problem. Meanwhile, Shao et al. [18] addressed the global finite-time tracking of robot manipulators. Motivated by the aforementioned results, we will investigated the finite-time DSC for a class of uncertain high-order nonlinear systems with mismatched nonlinear functions.

In this paper, HOSM observer is employed to handle mismatched uncertain functions in high-order low-triangular nonlinear systems. As a result, no function approximators are needed and thus the computation burden is significantly reduced. Different from traditional DSC method, second-order sliding mode will be designed to achieve finite-time convergence of tracking errors. Furthermore, the whole closed-loop stability is also proved to be finite-time.

The main contributions of this paper are summarized as follows. 1) The high-order mismatched uncertain functions are viewed as disturbance signals, which are handled by HOSM observer rather than function approximators. The finite-time feature of HOSM observer is attractive and allows finite-time DSC to be defined, which is different from traditional DSC. 2) A novel terminal sliding surface is designed in each step of iteration in DSC design. The developed sliding surface is also finite-time convergence with settling time given explicitly. Thus, the whole closed-loop is proved to be finite-time stable.

The rest of this paper is organized as follows. Section II provides problem formulation and some preliminaries about HOSM observer. Then, finite-time DSC design is given in Section III. In Section IV, stability analysis of the whole closed-loop systems and finite-time convergence of all signals are shown in Lyapunov method. In Section V, the proposed method is validated by two simulation examples with satisfactory results. Finally, Section VI concludes this paper.

2. Problem formulation and preliminaries

This section begins with providing system description and establishing the control objective. Then, some preliminaries about HOSM observer are recalled to facilitate the finite-time control design.

2.1. System description

Consider a strict-feedback low-triangular nonlinear system with single-input and single-output (SISO) in the form of

$$\begin{cases} \dot{x}_i = f_i(\bar{x}_i, t) + x_{i+1}, \quad i = 1 \ \cdots \ n \\ \dot{x}_n = f_n(\bar{x}_n, t) + g_n(\bar{x}_n)u \end{cases} \tag{1}$$

where $x = [x_1, \ \cdots, \ x_n]^T$ is the state vector, u is the control input, y is the controlled output, $f_i(\bar{x}_i)$, $i = 1, \ \cdots, \ n$ is the disturbance with at least ϱ_ith order bounded derivatives, and $g_n(\bar{x}_n)$ is smooth function of $\bar{x}_n$. Suppose that $f_i^{(\varrho_i)}$ has a Lipshitz constants L_i.

In order to design second-order sliding surface, (1) is rewritten as

$$\begin{cases} \dot{x}_{j_1} &= f_{j_1}(\bar{x}_{j_1}, t) + x_{j_2} \\ \dot{x}_{j_2} &= f_{j_2}(\bar{x}_{j_2}, t) + x_{(j+1)_1} \\ \cdots & \\ \dot{x}_n &= f_n(\bar{x}_n, t) + g_n(\bar{x}_n)u \\ y &= x_1 \end{cases} \tag{2}$$

where $j = 1, \cdots, m$ with $m = \text{round}(n/2)$.

For system (1) which can be written as (2), the control objective is to design finite-time DSC to make the output signal y track a reference signal x_d despite the existing disturbance caused by mismatched uncertain signals f_i.

2.2. High-order sliding mode observer

To deal with unknown functions f_i in (1), define a high-order sliding mode(HOSM) differentiator[19, 20] as

$$\begin{cases} \dot{z}_0^i &= \upsilon_0^i + x_{i+1}, \ \dot{z}_1^i = \upsilon_1^i, \cdots, \ \dot{z}_{\rho_i - 1}^i = \upsilon_{\rho_i - 1}^i, \ \dot{z}_{\rho_i}^i = \upsilon_{\rho_i + 1}^i, \\ \upsilon_0^i &= -\kappa_0^i L_i^{\frac{1}{\rho_i + 1}} |z_0^i - x_i|^{\frac{\rho_i}{\rho_i + 1}} \text{sign}(z_0^i - x_i) + z_1^i, \\ \upsilon_1^i &= -\kappa_1 L_i^{\frac{1}{\rho_i}} |z_1^i - \upsilon_0^i|^{\frac{\rho_i - 1}{\rho_i}} \text{sign}(z_1^i - \upsilon_0^i) + z_2^i, \\ & \cdots \\ \upsilon_{\varrho_i}^i &= -\kappa_{\varrho_i}^i L_i^{\frac{1}{2}} |z_{\rho_i}^i - \upsilon_{\rho_i - 1}^i|^{\frac{1}{2}} \text{sign}(z_{\rho_i}^i - \upsilon_{\varrho_i - 1}^i) + z_{\rho_i}^i, \\ \upsilon_{\varrho_i + 1}^i &= -\kappa_{\varrho_i}^i L_i \text{sign}(z_{\rho_i + 1}^i - \upsilon_{\varrho_i}^i) \\ y &= x_1 \end{cases} \tag{3}$$

where x_{i+1} denotes $g_n(\bar{x}_n)u$ for the simplicity of expression, ϱ_i is the order of differentiator, $\kappa_\iota^i > 0 (\iota = 0, 1, \cdots, \varrho_i; \ i = 1, \cdots, n)$ are the coefficients of the differentiator to be designed, and $z_0^i, \cdots, z_\iota^i$ are the estimates of $x_i, \ f_i, \ \dot{f}_i, \cdots, f_i^{(\varrho_i)}$, respectively.

From (1) and (3), it is obtained that the estimation errors are governed by

$$\begin{cases} \dot{\eta}_0^i &= -\kappa_0^i L_i^{\frac{1}{\rho_i + 1}} |z_0^i - x_i|^{\frac{\rho_i}{\rho_i + 1}} \text{sign}(\eta_0^i) \\ \dot{\eta}_\iota^i &= -\kappa_{\varrho_i - 1}^i L_i^{\frac{1}{2}} |z_{\rho_i - 1}^i - \upsilon_{\rho_i - 2}^i|^{\frac{1}{2}} \text{sign}(\eta_\iota^i - \dot{\eta}_{\iota - 1}^i) \\ \dot{\eta}_{\varrho_i + 1}^i &\in -\kappa_{\varrho_i}^i L_i \text{sign}(\eta_{\varrho_i + 1}^i - \dot{\eta}_{\varrho_i}^i) + [-L_i, L_i] \end{cases} \tag{4}$$

where the estimation errors are defined as $\eta_0^i = z_0^i - x_i$, $\eta_\iota^i = z_\iota^i - f_i^{(\iota)}$. It has been proved that the observer error system (4) is finite-time stable [21], which implies that there is a finite time such that $\eta_\iota^i = 0$.

3. Controller design

To facilitate the design procedure, we first denote the tracking error signals as

$$\begin{aligned} e_{j1} &= x_{j1} - \vartheta_{j-1}, \\ e_{j2} &= x_{j2} - \dot{\vartheta}_{j-1}, \end{aligned} \tag{5}$$

where ϑ_0 denotes $\vartheta_0 = x_d$.

The k^{th} $(1 \le k \le m-1)$ error surface is defined as

$$s_k = e_{k1} + \frac{1}{\lambda_k}(e_{k2} + {z_1}^{2k-1})^{p_k}. \tag{6}$$

where λ_k is positive design parameter, and $p_k = \dfrac{q_{k1}}{q_{k2}}$ with $q_{k2} > q_{k1}$ being positive odd integers.

3.1. Step 1:

From (6), define the first error surface as

$$s_1 = e_{11} + \frac{1}{\lambda_1}(e_{12} + z_1^1)^{p_1}, \tag{7}$$

where e_{11}, e_{12} are defined as $e_{11} = x_{11} - x_d$, $e_{12} = x_{12} - \dot{x}_d$. According to (2), (5) and (6), the time derivatives of the tracking error signals e_{11} and e_{12} are

$$\begin{aligned} \dot{e}_{11} &= x_{12} + f_{11} - \dot{x}_d, \\ \dot{e}_{12} &= f_{12} + x_{21} - \ddot{x}_d = f_{12} + e_{21} + \vartheta_1 - \ddot{x}_d = f_{12} + s_2 - \tfrac{1}{\lambda_2}\tilde{e}_{22}^{p_2} + \vartheta_1 - \ddot{x}_d, \end{aligned} \tag{8}$$

where $\tilde{e}_{22} = e_{22} + z_1^3$.

Consider a Lyapunov candidate function as

$$V_1 = \frac{1}{2}s_1^2 \tag{9}$$

with s_1 defined as in (7).

Then, to stabilize dynamics in sliding surface (7), an intermediate virtual control is defined as

$$\vartheta_1 = -[\frac{\lambda_1}{p_1}\tilde{e}_{12}^{2-p_1} + z_2^1 + z_1^2 + K_{11}s_1 + K_{12}\mathrm{sign}(s_1)|s_1|^\alpha], \tag{10}$$

where K_{11}, K_{12}, $0 < \alpha < 1$ are design parameters and α is odd. z_2^1 and z_1^2 are estimates of $\dot{f}_{11}$ and f_{12}, respectively.

According to (7), (8) and (10), the time derivatives of s_1 can be computed as

$$\begin{aligned} \dot{s}_1 &= \dot{e}_{11} + \frac{p_1}{\lambda_1}(e_{12} + z_1^1)^{p_1-1}(\dot{e}_{12} + z_2^1) = f_{11} + x_{12} - \dot{x}_d + \tfrac{p_1}{\lambda_1}\tilde{e}_{12}^{p_1-1}(f_{12} + s_2 - \tfrac{1}{\lambda_2}\tilde{e}_{22}^{p_2} + \vartheta_1 - \ddot{x}_d + {z_2}^1) \\ &= -\tfrac{p_1}{\lambda_1}\tilde{e}_{12}^{p_1-1}[K_{11}s_1 + K_{12}\mathrm{sign}(s_1)|s_1|^\alpha - \eta_1^2 - s_2 + \tfrac{1}{\lambda_2}\tilde{e}_{22}^{p_2} + \ddot{x}_d] - \eta_1^1 \end{aligned} \tag{11}$$

with $\tilde{e}_{12} = e_{12} + z_1^1$.

Then, the derivative of V_1 is calculated as

$$\dot{V}_1 = s_1\dot{s}_1 = -\frac{p_1}{\lambda_1}K_{11}\tilde{e}_{12}^{p_1-1}s_1^2 - \frac{p_1}{\lambda_1}K_{12}\tilde{e}_{12}^{p_1-1}|s_1|^{\alpha+1} + \frac{p_1}{\lambda_1}\tilde{e}_{12}^{p_1-1}s_1(\eta_1^2 - \tfrac{1}{\lambda_2}\tilde{e}_{22}^{p_2} - \ddot{x}_d) - s_1\eta_1^1 + \frac{p_1}{\lambda_1}\tilde{e}_{12}^{p_1-1}s_1s_2, \tag{12}$$

where K_{11} and K_{12} should be designed to make $\dot{V}_1$ negative definite.

It is easy to check that

$$s_1(\eta_1^2 - \tfrac{1}{\lambda_2}\tilde{e}_{22}^{p_2} - \ddot{x}_d) \le \frac{3}{2}s_1^2 + \frac{1}{2}(\eta_1^2)^2 + \frac{1}{2}\tfrac{1}{\lambda_2^2}\tilde{e}_{22}^{2p_2} + \frac{1}{2}\ddot{x}_d^2, \quad s_1\eta_1^1 \le \frac{1}{2}s_1^2 + \frac{1}{2}(\eta_1^1)^2. \tag{13}$$

Then, by substituting (13) into (12), one has

$$\dot{V}_1 \le -[\frac{p_1}{\lambda_1}\tilde{e}_{12}^{p_1-1}(K_{11} - \frac{3}{2}) - \frac{1}{2}]s_1^2 - \frac{p_1}{\lambda_1}K_{12}\tilde{e}_2^{p_1-1}s_1^{\alpha+1} + \frac{1}{2}[(\eta_1^2)^2 + (\eta_1^1)^2 + (\frac{1}{\lambda_2}\tilde{e}_{22}^{p_2})^2 + \ddot{x}_d^2] + \frac{p_1}{\lambda_1}\tilde{e}_{12}^{p-1}s_1s_2. \tag{14}$$

Furthermore, by choosing $K_{11} > \dfrac{\lambda_1}{2p_1}\tilde{e}_{12}^{1-p_1} + \dfrac{3}{2}$, one obtains

$$\dot{V}_1 \le -\rho_{11}s_1^2 - \rho_{12}s_1^{\alpha+1} + \varsigma_1 + \frac{p_1}{\lambda_1}\tilde{e}_{12}^{p_1-1}s_1s_2 \tag{15}$$

with

$$\rho_{11} = \frac{p_1}{\lambda_1}\tilde{e}_{12}^{p_1-1}(K_{11} - \frac{3}{2}) - \frac{1}{2}, \quad \rho_{12} = \frac{p_1}{\lambda_1}K_{12}\tilde{e}_{12}^{p_1-1}, \quad \varsigma_1 = \frac{1}{2}[(\eta_1^2)^2 + (\eta_1^1)^2 + (\tfrac{1}{\lambda_2}\tilde{e}_{22}^{p_2})^2 + \ddot{x}_d^2] \tag{16}$$

which are greater than zero.

From (2) and (5), it is obtained that

$$\dot{e}_{11} = e_{12} + f_{12}, \tag{17}$$

where f_{12} is estimated by HOSM observer (3).

Substituting (17) into (7) obtains

$$s_1 = e_{11} + \frac{1}{\lambda_1}(\dot{e}_{11} + \eta_1^1)^{p_1}. \tag{18}$$

Since the disturbance estimation error η_1^1 converge to zero in a finite-time, (18) reduced to

$$\lambda_1 e_{11} + \dot{e}_{11}^{p_1} = 0 \tag{19}$$

which represents a sliding motion in the dynamic surface s_1.

It has been shown that the time for terminal attractor $e_{11} = 0$ reaching zero [22] is

$$t_1 = \frac{p_1 e_{11}^{\frac{p_1-1}{p_1}}(0)}{\lambda_1(1-p_1)}. \tag{20}$$

3.2. Step k $(2 \leq k \leq m-1)$**:**

From (5), one obtains

$$\begin{aligned} e_{k_1} &= x_{k_1} - \vartheta_{k-1} \\ e_{k_2} &= x_{k_2} - \dot{\vartheta}_{k-1}. \end{aligned} \tag{21}$$

The kth error surface is defined as

$$s_k = e_{k_1} + \frac{1}{\lambda_k}(e_{k_2} + z_1^{2k-1})^{p_k}, \tag{22}$$

where λ_k is positive constant, $p_k = \frac{q_{k1}}{q_{k2}}$ with $q_{k2} > q_{k1}$ being positive odd integers.

The derivative of s_k along system dynamics is

$$\dot{s}_k = \dot{e}_{k_1} + \frac{p_k}{\lambda_k}(e_{k_2} + z_1^{2k-1})^{p_k-1}(\dot{e}_{k2} + z_2^{2k-1}). \tag{23}$$

Consider a Lyapunov candidate function as

$$V_k = \frac{1}{2}s_k^2 \tag{24}$$

with the derivative being

$$\dot{V}_k = s_k \dot{s}_k. \tag{25}$$

To stabilize dynamics in sliding surface (22), the kth virtual intermediate control signal is given as

$$\vartheta_k = -[\frac{\lambda_k}{p_k}(e_{k_2} + z_1^{2k-1})^{1-p_k}(\tilde{e}_{k2} + \frac{\lambda_{k-1}}{p_{k-1}}\tilde{e}_{k-12}^{p_{k-1}-1}s_{k-1}) + z_1^{2k} + z_2^{2k-1} + K_{k_1}s_k + K_{k2}\text{sign}(s_k)|s_k|^{\alpha}]. \tag{26}$$

Similar to Step 1, it is proved that $\dot{V}_1$ satisfies

$$\dot{V}_k \leq -\rho_{k1}s_k^2 - \rho_{k2}s_k^{\alpha+1} + \varsigma_k + \frac{p_k}{\lambda_k}\tilde{e}_{k2}^{p_k-1}s_k s_{k+1} - \frac{p_{k-1}}{\lambda_{k-1}}\tilde{e}_{k-1\ 2}^{p_{k-1}-1}s_{k-1}s_k \tag{27}$$

with

$$\rho_{k1} = \frac{p_k}{\lambda_k}\tilde{e}_{k2}^{p_k-1}(K_{k1} - \frac{3}{2}) - \frac{1}{2}, \quad \rho_{k2} = \frac{p_k}{\lambda_k}K_{k2}\tilde{e}_{k2}^{p_k-1}, \quad \varsigma_1 = \frac{1}{2}[(\eta_1^{2k})^2 + (\eta_1^{2k-1})^2 + (\frac{1}{\lambda_{k+1}}\tilde{e}_{k+12}^{p_k+1})^2] \tag{28}$$

which are greater than zero.

From (2) and (21), it is calculated that

$$\dot{e}_{k1} = e_{k2} + f_{k1}. \tag{29}$$

Substituting (29) into (23) yields

$$s_k = e_{k1} + \frac{1}{\lambda_k}(\dot{e}_{k1} + \eta_1^{k1})^{p_k}. \tag{30}$$

Since the disturbance estimation error η_1^{2k-1} converge to zero in a finite-time, (30) will reduce to

$$\lambda_k e_{k1} + \dot{e}_{k1}^{p_k} = 0 \tag{31}$$

which represents the motion of the kth sliding surface s_k.

It follows that

$$t_k = \frac{p_k e_{k1}^{\frac{p_k-1}{p_k}}(0)}{\lambda_k(1-p_k)}. \tag{32}$$

3.3. Step m:

This is the last step of the controller design procedure. It is divided into two cases according to the system order n. If system n is even, the last sliding mode is defined as

$$s_m = e_{m1} + \frac{1}{\lambda_m}(e_{m2} + z_1^{2m-1})^{p_m}, \tag{33}$$

where λ_m is positive constant, $p_m = \frac{q_{m1}}{q_{m2}}$ with q_{m1} and q_{m2} being positve odd integers.

Differentiating (33) along (1) and (3) obtains

$$\dot{s}_m = \dot{e}_{m1} + \frac{p_m}{\lambda_m}(e_{m2} + z_1^{2m-1})^{p_m-1}(\dot{e}_{m1} + z_2^{2m-1}). \tag{34}$$

Then, the actual control signal is given as

$$u = -g^{-1}(\bar{x}_n)[\frac{\lambda_m}{p_m}(\tilde{e}_{m2})^{1-p_m}(\tilde{e}_{m2} + \frac{\lambda_{m-1}}{p_{m-1}}\tilde{e}_{m-12}^{p_{m-1}-1}s_{m-1}) + z_1^{2m} + z_2^{2m-1} + K_{k_1}s_k + K_{m2}\text{sign}(s_k)|s_k|^{\alpha}], \tag{35}$$

with K_{m1}, K_{m2} are positive control gains, $\tilde{e}_{m2} = e_{m_2} + z_1^{2m-1}$.

The last Lyapunov candidate function is $V_m = \frac{1}{2}s_m^2$ with derivative as

$$\dot{V}_m = s_m\dot{s}_m \tag{36}$$

satisfying

$$\dot{V}_m \leq -\rho_{m1}s_m^2 - \rho_{m2}s_m^{\alpha+1} + \varsigma_m - \frac{p_{m-1}}{\lambda_{m-1}}\tilde{e}_{m-1\,2}^{p_{m-1}-1}s_{m-1}s_m \tag{37}$$

with

$$\rho_{m1} = \frac{p_m}{\lambda_m}\tilde{e}_{m2}^{p_m-1}(K_{m1} - \frac{3}{2}) - \frac{1}{2}, \quad \rho_{m2} = \frac{p_m}{\lambda_m}K_{m2}\tilde{e}_{m2}^{p_m-1}, \quad \varsigma_m = \frac{1}{2}[(\eta_1^n)^2 + (\eta_1^{2m-1})^2], \tag{38}$$

which are greater than zero.

From (1), we have

$$\dot{e}_{m1} = e_{m2} + f_{m1}. \tag{39}$$

Substituting (39) into (33) yields

$$s_m = e_{m1} + \frac{1}{\lambda_m}(\dot{e}_{m1} + \eta_1^{m1})^{p_m}. \tag{40}$$

Since the disturbance estimation error η_1^{m1} converge to zero in a finite-time, (40) will induce to

$$\lambda_m e_{m1} + \dot{e}_{m1}^{p_m} = 0 \tag{41}$$

which means terminal attractor $e_{m1} = 0$ reachs to zeros in

$$t_m = \frac{p_m e_{m1}^{\frac{p_{m-1}}{p_m}}(0)}{\lambda_m(1-p_m)}. \tag{42}$$

For the case when system order n is odd, the last error surface is defined as

$$s_m = e_m = x_n - \vartheta_m. \tag{43}$$

Differentiate (43) along (1) yields

$$\dot{s}_m = f_n(\bar{x}_n, t) + g_n(\bar{x}_n)u - \dot{\vartheta}_m. \tag{44}$$

The actual control law is given as

$$u = -g_n^{-1}(\bar{x}_n)[K_{n1}e_n + z_1^n + K_{n2}\text{sign}(e_n)|e_n|^\alpha - \frac{\lambda_{m-1}}{p_{m-1}}\tilde{e}_{m-12}^{p_{m-1}-1}s_{m-1} - \dot{\vartheta}_m] \tag{45}$$

where K_{n1} and K_{n2} are positive design parameters.

Then, the last Lyapunov candidate function is chosen as

$$V_m = \frac{1}{2}s_m^2 \tag{46}$$

with the derivative as

$$\dot{V}_m = -K_{m1}s_m^2 - K_{m2}|s_m|^{\alpha+1} - \eta_1^m s_m - \eta_{m-1,2}s_m - \frac{\lambda_{m-1}}{p_{m-1}}\tilde{e}_{m-12}^{p_{m-1}-1}s_{m-1}s_m \tag{47}$$

satisfying

$$\dot{V}_m \leq -\rho_{m1}s_m^2 - K_{m2}s_m^{\alpha+1} + \varsigma_m - \frac{p_{m-1}}{\lambda_{m-1}}\tilde{e}_{m-1\,2}^{p_{m-1}-1}s_{m-1}s_m \tag{48}$$

with

$$\rho_{m1} = K_{m1} - \frac{1}{2}, \quad \rho_{m2} = K_{m2}, \quad \varsigma_m = \frac{(\eta_1^{m1})^2}{2}, \tag{49}$$

which are greater than zero.

In the coming section, we will prove that, by properly choosing the design parameters K_{k1}, K_{k2}, $k = 1, \cdots, m$, n, the whole closed-loop system is finite-time convergence.

4. Stability analysis

We have the following theorem to summarize the main results of our proposed finite-time control scheme for uncertain nonlinear systems.

Theorem 1 *For system (1) with mismatched uncertain functions f_i , if the virtual control signals are designed as (10), (26), and actual control signal is provided as (35), the whole closed-loop system is finite-time stable and all signals are SGUUB. Furthermore, the tracking errors converge to zero in finite-time.*

Proof By virtue of (9), (24) and (36),we choose the Lyapunov candidate function

$$V = \sum_{j=1}^{m} V_j. \tag{50}$$

From (15), (27) and (37), it is obtained that the derivative of (50) satisfies

$$\dot{V} \leq -\rho_1 V - \rho_2 V^{\frac{\alpha+1}{2}} + \varsigma, \tag{51}$$

where K_1, K_2 and ς are defined as

$$\rho_1 = \min_{1\leq j\leq m}\{\rho_{j1}\}, \quad \rho_2 = \min_{1\leq j\leq m}\{\rho_{j2}\}, \quad \varsigma = \sum_{j=1}^{m}\varsigma_j. \tag{52}$$

Since the disturbance estimation errors η_1^i, $i = 1, \cdots, n$ converge to zero in a finite-time, (51) then reduces to

$$\dot{V} + \rho_1 V + \rho_2 V^{\beta} \leq 0 \tag{53}$$

with $\beta = \frac{\alpha+1}{2}$. Since $V^{\beta}(t) > 0$, (53) can be rewritten as

$$V^{-\beta}\dot{V} + \rho_1 V^{1-\beta}(t) + \rho_2 \leq 0, \quad \forall \ t \geq t_0. \tag{54}$$

Setting $\xi = V^{1-\beta}(t)$ obtains

$$\dot{\xi} = -(1-\beta)V^{-\beta}(t)\dot{V}(t). \tag{55}$$

Multiplying $1-\beta$ on both side of (54) and substituting (55) into (54), one obtains

$$\dot{\xi} \leq -(1-\beta)(\rho_1\xi + \rho_2). \tag{56}$$

Integrating both side of (56) from t_0 to t yields

$$\ln(\frac{\rho_1\xi(t)+\rho_2}{\rho_1\xi(t_0)+\rho_2}) \leq -\rho_1(1-\beta)(t-t_0) \tag{57}$$

which can be written as

$$\xi(t) \leq (\xi(t_0) + \frac{\rho_2}{\rho_1})e^{-\rho_1(1-\beta)(t-t_0)} - \frac{\rho_2}{\rho_1}. \tag{58}$$

Then, substituting $\xi(t) = V^{1-\beta}(t)$ and $\xi(t_0) = V^{1-\beta}(t_0)$ into (58) obtains

$$V^{1-\beta}(t) \leq (V^{1-\beta}(t_0) + \rho)e^{-\rho_1(1-\beta)(t-t_0)} - \rho \tag{59}$$

with $\rho = \frac{\rho_2}{\rho_1}$.

Finally, it can be concluded that $V(t) \equiv 0, \quad \forall > t_s$ with t_s defined as

$$t_s = t_0 + \frac{1}{\rho_1(1-\beta)}\ln\frac{V^{1-\beta}(t_0)+\rho}{\rho}. \tag{60}$$

This completes the proof.

5. Simulation studies

To illustrate our proposed finite-time control scheme, consider a third-order low-triangular nonlinear system in the form of

$$\begin{cases} \dot{x}_1 &= f_1(x_1, x_2) + x_2 \\ \dot{x}_2 &= f_2(x_1, x_2, x_3) + x_3 \\ \dot{x}_3 &= f_3(x_1, x_2, x_3) + g_3 u \end{cases} \tag{61}$$

where f_1, f_2 and f_3 are unknown smooth functions with mismatched conditions and $g_3 = 1$. The control objective is to design a feedback law u to achieve that the output of the closed-loop system asymptotically tracks a reference signal $x_d = \sin(t)$ in finite time. In this paper, it is assumed that

$$\begin{aligned} f_1(x_1, x_2) &= 2x_1 \sin(x_1) + x_1^2 x_2, \\ f_2(x_1, x_2, x_3) &= x_1^2 + x_1 x_2 + x_2 \cos(x_1) + \frac{x_2}{1 + x_3^2}, \\ f_3(x_1, x_2, x_3) &= x_1 x_3 + \frac{1}{1 + x_2^2} + x_3 \sin(x_2). \end{aligned} \tag{62}$$

To handle the mismatched unknown functions, a third-order HOSM is defined as

$$\begin{cases} \dot{z}_0^1 &= \upsilon_0^1 + x_2, \ \dot{z}_1^1 = \upsilon_1^1, \ \dot{z}_2^1 = \upsilon_2^1, \\ \upsilon_0^1 &= -\kappa_0^1 L_1^{\frac{1}{3}} |z_0^1 - x_1|^{\frac{2}{3}} \text{sign}(z_0^1 - x_1) + z_1^1 \\ \upsilon_1^1 &= -\kappa_1^1 L_1^{\frac{1}{2}} |z_1^1 - \upsilon_0^1|^{\frac{1}{2}} \text{sign}(z_1^1 - \upsilon_0^1) + z_2^1 \\ \upsilon_2^1 &= -\kappa_2^1 L_1 \text{sign}(z_2^1 - \upsilon_1^1) \end{cases} \tag{63}$$

where $z_0^1 = \hat{x}_1$, $z_1^1 = \hat{f}_1$, and $z_2^1 = \hat{\dot{f}}_1$ denote the estimates of x_1, f_1, and $\dot{f}_1$, respectively.

Similarly, two second-order HOSM are designed as follows.

$$\begin{cases} \dot{z}_0^2 &= \upsilon_0^2 + x_3, \ \dot{z}_1^2 = \upsilon_1^2, \ \dot{z}_2^2 = \upsilon_2^2, \\ \upsilon_0^2 &= -\kappa_0^2 L_2^{\frac{1}{2}} |z_0^2 - x_2|^{\frac{1}{2}} \text{sign}(z_0^2 - x_2) + z_1^2 \\ \upsilon_1^2 &= -\kappa_1^2 L_2 \text{sign}(z_1^2 - \upsilon_1^2) \end{cases} \tag{64}$$

where $z_0^2 = \hat{x}_2$ and $z_1^2 = \hat{f}_2$ denote the estimates of x_2 and $\hat{f}_2$, respectively.

$$\begin{cases} \dot{z}_0^3 &= \upsilon_0^3 + g_3 u, \ \dot{z}_1^3 = \upsilon_1^3, \ \dot{z}_2^3 = \upsilon_2^3, \\ \upsilon_0^3 &= -\kappa_0^3 L_3^{\frac{1}{2}} |z_0^3 - x_3|^{\frac{1}{2}} \text{sign}(z_0^3 - x_3) + z_1^3 \\ \upsilon_1^3 &= -\kappa_1^3 L_3 \text{sign}(z_1^3 - \upsilon_1^3). \end{cases} \tag{65}$$

with $z_0^3 = \hat{x}_3$ and $z_1^3 = \hat{f}_3$ denote the estimates of x_3 and $\hat{f}_3$, respectively.

Then, define the sliding surface as

$$s_1 = e_{11} + (e_{12} + z_1^1)^{p_1} \tag{66}$$

with $e_{11} = x_{11} - x_d$ and $e_{12} = x_{12} - \dot{x}_d$. As detailed in Step 1 of the controller design procedure, an intermediate virtual control signal is given as

$$\vartheta_1 = -[\frac{\lambda_1}{p_1} \tilde{e}_{12}^{2-p_1} + z_2^1 + z_1^1 + K_{11} s_1 + K_{12} \text{sign}(s_1) |s_1|^{\alpha}] \tag{67}$$

with $\tilde{e}_{12} = e_{12} + z_1^1$. Moreover, the actual control signal is provided as

$$u = -g_{21}^{-1}[K_{21}e_{21} + z_1^3 + K_{22}\text{sign}|e_3|^{\alpha} - \dot{\vartheta}_1] \tag{68}$$

with $e_{21} = x_{21} - \vartheta_1$.

The values of design parameters used in simulation are listed as in Table 1.

Table 1. Designed parameters of finite-time DSC

HOSM observer 1	$\kappa_0^1 = 10$	$\kappa_1^1 = 8$	$\kappa_2^1 = 20$	$L_1 = 15$
HOSM observer 2	$\kappa_0^2 = 10$	$\kappa_1^2 = 13$	x	$L_2 = 10$
HOSM observer 3	$k_0^3 = 10$	$\kappa_1^3 = 10$	x	$L_3 = 10$
s_1	$\lambda_1 = 3$	$q_1 = 5$	$q_2 = 3$	$p_1 = 5/3$
ϑ_1	$K_{11} = 30$	$K_{12} = 0.15$	$\alpha_1 = 2/3$	x
u	$K_{21} = 3$	$K_{22} = 0.25$	$\alpha_2 = 2/3$	x

The simulation results are depicted in Figures 1–3. Figure 1 depicts the control performance under control law with two different types of disturbances. The HOSM performance of estimating unknown system status and uncertain functions are shown in Figure 2. The corresponding estimate errors are given in Figure 3, which are all finite-time convergence. To summarize, the proposed scheme combining the modifed DSC and HOSM observer successfully achieves finite-time feedback control problem of (61) with satisfactory results.

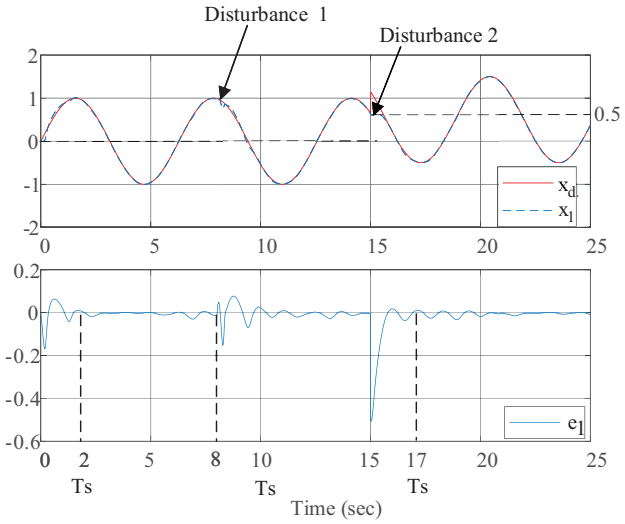

Figure 1. Output signal (dashed line) tracks reference signal (solid line) in the upper subfigure with convergence error in the lower subfigure.

From comparison, the NN-based control method proposed in is also employed to control (61). The adaptive NN controller used in simulation is in the form of

$$\vartheta_1 = -c_1e_1 - \hat{W}_1^T\phi(Z_1) + \dot{x}_d, \quad \vartheta_2 = -c_2e_2 - \hat{W}_2^T\phi(Z_2) + \dot{\vartheta}_1, \quad u_N = -c_3e_3 - \hat{W}_3^T\phi(Z_3) + \dot{\vartheta}_2 \tag{69}$$

where tracking errors are defined as $e_1 = x_1 - x_d$, $e_2 = x_2 - \vartheta_1$, $e_3 = x_3 - \vartheta_2$, NN input vectors are

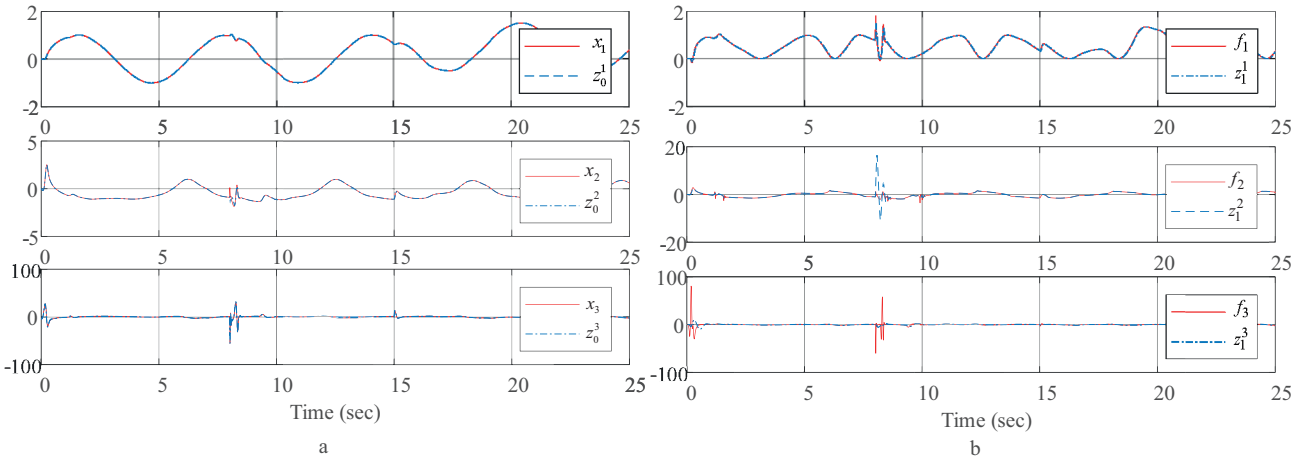

Figure 2. (a)The estimate performance of HOSMs with solid line being the real states and dashed line being their estimation.(b)The estimate performance of HOSMs with solid line being the real uncertain functions and dashed line being their estimation.

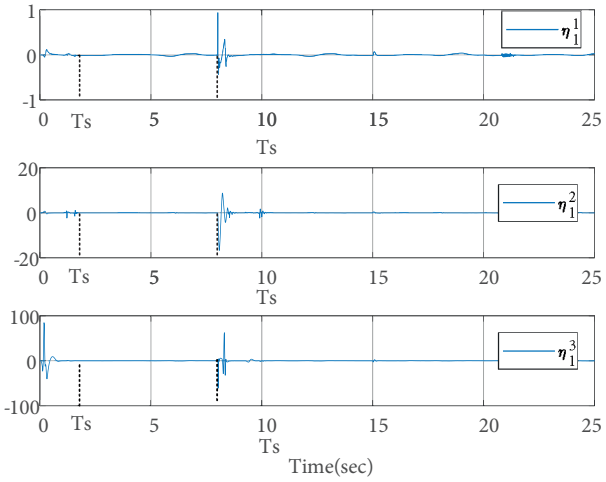

Figure 3. Finite-time convergence for estimate errors of HOSM observer.

defined as $Z_1 = [x_1,\ x_2]$, $Z_2 = [x_1,\ x_2,\ x_3]$, $Z_3 = [x_1,\ x_2,\ x_3]$, and the adaptive laws are

$$\dot{\hat{W}}_i = \Gamma_i^{-1}(e_i\phi(Z_i) - \sigma_i\hat{W}_i), \quad i = 1, 2, 3, \tag{70}$$

with $\phi(Z_i)$ being the Gaussian functions. The parameters used in simulation are given as in Table 2.

Table 2. Designed parameters of adaptive NN controller

NN 1	$\Gamma_1 = 15$	$\sigma_1 = 0.02$	$N_1 = 25$
NN 2	$\Gamma_2 = 11$	$\sigma_2 = 0.02$	$N_2 = 35$
NN 3	$\Gamma_3 = 3$	$\sigma_3 = 0.5$	$N_3 = 35$
Gains	$c_1 = 13$	$c_2 = 15$	$c_3 = 12$

The simulation results are depicted in Figures 4–6. From Figure 4, it is observed that the tracking performance is also acceptable. However, from Figure 5 , we see that the estimate performance of NNs is not so satisfying. By comparing Figure 2 and Figure 5 with corresponding errors in Figure 3 and Figure 5, it is concluded that the designed HOSM observer is superior to NN in online estimating mismatched uncertain nonlinear functions in system (1). In addition, norms of NN weights are depicted in Figure 6 which are also bounded.

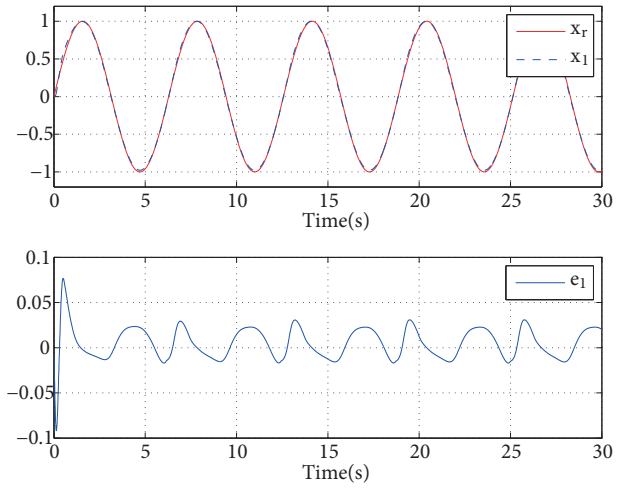

Figure 4. Tracking performance using adaptive NN controller with solid line being the reference signal and dashed line being system output in the upper subfigure.

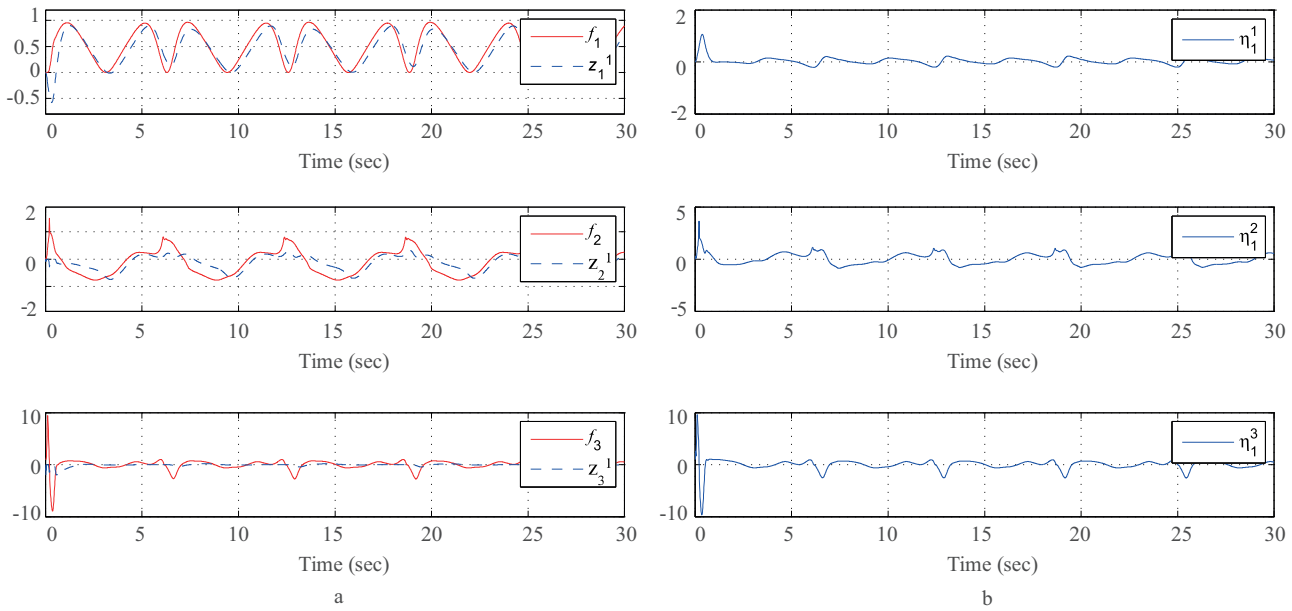

Figure 5. (a)The estimate performance of NNs with solid line being the real unknown functions and dashed line being their estimation.(b)The estimate errors of NN approximators.

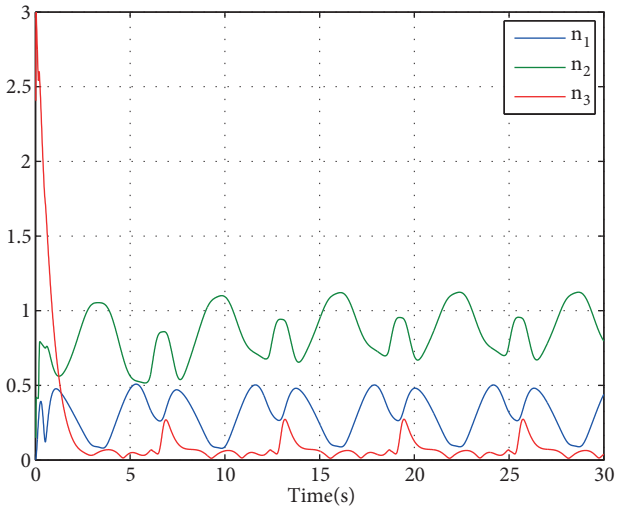

Figure 6. Norms of the employed NNs.

To evaluate the control performance quantitatively, four indices are adopted as:

$$IAE = \int |e_1(t)|dt, \quad ITAE = \int t|e_1(t)|dt, ISE = \int {e_1}^2(t)dt, \quad ITDE = \int t{e_1}^2(t)dt. \tag{71}$$

and the results of estimate performance of e_1, η_1^1, η_1^2 and η_1^3 are shown in Table 3.

Table 3. Observers performance analysis

	IAE		ITAE		ISE		ISDE	
	NN	HOSM	NN	HOSM	NN	HOSM	NN	HOSM
e_1	36.23	18.44	100.54	30.85	2.89	1.81	4.43	1.03
η_1^1	124.17	12.70	466.58	43.31	28.02	0.41	86.33	0.85
η_1^2	327.67	74.03	$1.13 * 10^3$	165.97	213.46	54.60	607.79	68.51
η_1^3	$2.49 * 10^3$	$1.87 * 10^3$	$8.37 * 10^3$	$1.10 * 10^3$	$5.16 * 10^3$	$7.40 * 10^4$	$2.13 * 10^5$	$1.77 * 10^4$

It can be found from these results that the modified DSC via HOSM observer method is robustness for time-varying signals with good tracking performance.

6. Conclusion

In this paper, we reported a novel finite DSC method for tracking control of uncertain nonlinear systems with mismatched unknown functions. By designing HOSM observer, the unknown functions and its derivatives were finite-time online obtained. Subsequently, second-order sliding surfaces with finite-time convergence were developed to allow finite-time controller design. Furthermore, finite-time DSC scheme of the whole-closed loop was provided in detail with stability analysis by Lyapunov method. The proposed approach do not need function approximators with fast convergence. Simulation results illustrated that, compared with the approximators-based adaptive methods, the proposed algorithm in this paper was more effective and applicable.

Acknowledgment

This work was supported by the National Natural Science Foundation of China under Grant 61703224, 61620304 and 21606141.

References

[1] Liu Y, Zeng Q, Tong S, Chen CLP, Liu L. Adaptive neural network control for active suspension systems with time-varying vertical displacement and speed constraints. IEEE Transactions on Industrial Electronics 2019; 66 (12): 9458-9466. doi: 10.1109/TIE.2019.2893847

[2] Yu J, Shi P, Lin C, Yu H. Adaptive neural command filtering control for nonlinear MIMO systems with saturation input and unknown control direction. IEEE Transactions on Cybernetics 2019; in press. doi: 10.1109/TCYB.2019.2901250

[3] Qiu J, Sun K, Wang T, Gao H. Observer-based fuzzy adaptive event-triggered control for pure-feedback nonlinear systems with prescribed performance. IEEE Transactions on Fuzzy Systems 2019; 27 (11): 2152-2162. doi: 10.1109/TFUZZ.2019.2895560

[4] Li K, Tong S. Observer-based finite-time fuzzy adaptive control for MIMO non-strict feedback nonlinear systems with errors constraint. Neurocomputing 2019; 314: 135-148. doi: 10.1016/j.neucom.2019.02.022

[5] Guo X, Yan W, Cui R. Event-triggered reinforcement learning-based adaptive tracking control for completely unknown continuous-time nonlinear systems. IEEE Transactions on Cybernetics 2019; in press. doi: 10.1109/TCYB.2019.2903108

[6] Guo X, Yan W, Cui R. Integral reinforcement learning-based adaptive NN Control for continuous-time nonlinear MIMO systems with unknown control directions. IEEE Transactions on Systems, Man, and Cybernetics: Systems 2019; in press. doi: 10.1109/TSMC.2019.2897221

[7] Pisano A, Usai E. Sliding mode control: A survey with applications in math. Mathematics and Computers in Simulation 2011; 81 (5): 954-979. doi: 10.1016/j.matcom.2010.10.003

[8] Shi S, Xu S, Zhang B, Ma Q, Zhang Z. Global second - order sliding mode control for nonlinear uncertain systems. International Journal of Robust and Nonlinear Control 2019; 29 (1): 224-237. doi: 10.1002/rnc.4385

[9] Tiwari P.M, Janardhanan S, Nabi M. Spacecraft anti-unwinding attitude control using second-order sliding mode. Asian Journal of Control 2018; 20 (1): 455-468. doi: 10.1002/asjc.1601

[10] Matraji I, Al-Durra A, Haryono A, Al-Wahedi K, Abou-Khousa M. Trajectory tracking control of skid-steered mobile robot based on adaptive second order sliding mode control. Control Engineering Practice 2018; 72: 167-176. doi: 10.1016/j.conengprac.2017.11.009

[11] Qiao L, Zhang W. Adaptive second-order fast nonsingular terminal sliding mode tracking control for fully actuated autonomous underwater vehicles. IEEE Journal of Oceanic Engineering 2019; 44 (2): 363-385. doi: 10.1109/JOE.2018.2809018

[12] Feng Y, Xue C, Han Q, Han F, Du J. Robust estimation for state-of-charge and state-of-health of lithium-ion batteries using integral-type terminal sliding-mode observers. IEEE Transactions on Industrial Electronics 2019; 67 (5): 4013-4023. doi: 10.1109/TIE.2019.2916389

[13] Wu X, Wang C, Hua S. Adaptive extended state observer-based nonsingular terminal sliding mode control for the aircraft skin inspection robot. Journal of Intelligent & Robotic Systems 2019; in press. doi: 10.1007/s10846-019-01067-1

[14] Bhat SP, Bernstein DS. Continuous finite-time stabilization of the translational and rotational double integrators. IEEE Transactions on Automatic Control 1998; 43 (5): 678-682. doi: 10.1109/9.668834

[15] Abooee A, Arefi MM. Robust finite-time stabilizers for a connected chain of nonlinear double-integrator systems. IEEE Systems Journal 2019; 13 (1): 833-841. doi: 10.1109/JSYST.2018.2851153

[16] Hou H, Yu X, Xu L, Rsetam KA, Cao Z. Finite-time continuous terminal sliding mode control of servo motor systems. IEEE Transactions on Industrial Electronics 2020; 67 (7): 5647-5656. doi: 10.1109/TIE.2019.2931517

[17] Lee J, Jin M, Kashiri N, Caldwell DG, Tsagarakis NG. Inversion-free force tracking control of piezoelectric actuatorsusing fast finite-time integral terminal sliding-mode. Mechatronics 2019; 57: 39-50. doi: 10.1016/j.mechatronics.2018.11.005

[18] Shao K, Zheng J, Huang K, Wang H, Man Z et al. Finite-time control of a linear motor positioner using adaptive recursive terminal sliding mode. IEEE Transactions on Industrial Electronics 2019; in press. doi: 10.1109/TIE.2019.2937062

[19] Levant A. Higher-order sliding modes, differentiation and output-feedback control. International Journal of Control 2003; 76 (9): 924-941. doi: 10.1080/0020717031000099029

[20] Chen Q, Shi L, Na J, Ren X, Nan Y. Adaptive echo state network control for a class of pure-feedback systems with input and output constraints. Neurocomputing 2018; 275: 1370-1382. doi: 10.1016/j.neucom.2017.09.083

[21] Shtessel Y, Shkolnikovb I, Levantc A. Smooth second-order sliding modes: Missile guidance application. Automatica 2007; 43 (8): 1470-1476. doi: 10.1016/j.automatica.2007.01.008

[22] Yin J, Khoo S, Man Z, Yu X. Finite-time stability and instability of stochastic nonlinear systems. Automatica 2011; 47 (12): 2671-2677. doi: 10.1016/j.automatica.2011.08.050